PLOS Climate

RESEARCH ARTICLE

Integrating machine learning to assess climate risks on reservoir's inflow and hydropower generation across West African basins

Franck Hervé Akaffou[1*], **Salomon Obahoundje**[2], **Arona Diedhiou**[3,4], **Kouakou Lazare Kouassi**[5], **Dior Diallo**[6], **Ernest Amoussou**[7], **Daniel Yamegueu**[8], **Eric Antwi Ofosu**[9]

1 Center for International Forestry Research and World Agroforestry (CIFOR– ICRAF), Abidjan, Côte d'Ivoire, **2** International Water Management Institute (IWMI), Accra, Ghana, **3** Institut des Géosciences de l'Environnement (IGE), Université Grenoble Alpes, Grenoble, France, **4** Laboratoire des Sciences de la Matière, de l'Environnement et de l'Énergie Solaire (LASMES), Université Félix Houphouët Boigny, Abidjan, Côte d'Ivoire, **5** Département des Sciences de la Terre, Université Jean Lorougnon Guédé, Daloa, Côte d'Ivoire, **6** Département Génie Rural, Ecole Nationale Supérieure d'Agriculture (ENSA), Université de Thiès, Thiès, Sénégal, **7** Département de Géographie Et Aménagement de Territoire, (DGAT/FLASH), Université de Parakou, Parakou, Bénin, **8** Laboratoire Energies Renouvelables et Efficacité Energétique (LabEREE), Institut International d'Ingénierie de l'Eau et de l'Environnement (2iE), Ouagadougou, Burkina Faso, **9** Regional Centre for Environmental Sustainability (RCEES), University of Energy and Natural Resources (UENR), Sunyani, Ghana

* F.Akaffou@cifor-icraf.org

Citation: Akaffou FH, Obahoundje S, Diedhiou A, Kouassi KL, Diallo D, Amoussou E, et al. (2026) Integrating machine learning to assess climate risks on reservoir's inflow and hydropower generation across West African basins. PLOS Clim 5(9): e0000986. https://doi.org/10.1371/journal.pclm.0000986

Editor: Muhammad Irfan Ashraf, University of Sargodha, PAKISTAN

Received: December 18, 2025

Accepted: June 16, 2026

Published: September 8, 2026

Data availability statement: The inflow and hydropower data used in this study were obtained from national institutions responsible for energy production and water resource management and are subject to access restrictions imposed by those institutions.

Abstract

This study presents a novel five-step ensemble machine learning approach to improve predictive accuracy in assessing climate change impacts on inflow patterns and hydropower generation across seven dam basins in West Africa. The methodology integrates precipitation and temperature using the multi-lag approach. An initial pool of fifteen machine learning models were evaluated, and top-performing models were selected for further refinement through iterative ensemble stacking and weak learner elimination. Historical analysis (1983–2014) utilized CHIRPS and CHIRTS datasets. Future projections employed twelve bias-adjusted CMIP6 models and their ensemble mean (EnsMean) under SSP1-2.6, SSP2-4.5, and SSP5-8.5 for the near (2036–2067) and far (2068–2099) futures. Results showed notable improvements in model accuracy and efficiency across layers, with R^2 and NSE exceeding 0.6 for all inflow simulations and for selected energy simulations (Bagre, Nangbeto, and Taabo). Projections indicated warming up to 4.5°C and spatially heterogeneous precipitation changes across basins and scenarios, with SSP5-8.5 projecting the most pronounced shifts. Inflow reductions are projected to reach up to 24% at Buyo and 13% at Nangbeto, while hydropower output may decline by up to 19% at Nangbeto and 58% at Taabo in the future. Conversely, Manantali and Taabo are projected to experience inflow increases, and Bagre may see energy gains of up to 42% under SSP5-8.5. These findings highlight heightened vulnerability, as well as contrasting opportunities across the region, underscoring the urgent need for adaptive management strategies,

The data are not publicly available but may be requested directly from the relevant data-holding organisations as follows: Côte d'Ivoire – Inflow and hydropower data: Compagnie Ivoirienne d'Electricité (CIE): info@cie.ci Ghana – Inflow and hydropower data: Electricity Company of Ghana (ECG): cnaayiku@ecggh.com Manantali (Senegal River) – Inflow data: Organisation de Mise en Valeur du fleuve Sénégal (OMVS): omvssphc@omvs.org; Hydropower data: Société de Gestion de l'Énergie de Manantali (SOGEM): info@sogem-omvs.org Bagre (Burkina Faso) – Inflow data: Direction Générale des Ressources en Eau (DGRE): dgre.dg@gmail.com; Hydropower data: Société Nationale d'Électricité du Burkina Faso (SONABEL): courrier@sonabel.bf Nangbeto (Togo/Benin) – Inflow data: Direction des Ressources en Eau du Togo: secretariat.sg@eau.gouv.tg; Hydropower data: Communauté Électrique du Bénin: info@cebnet.org The authors did not receive any special privileges in accessing these data that would not be available to other researchers upon request.".

Funding: This work was supported by the Responsible Artificial Intelligence Network for Climate Action in Africa (RAINCA) Consortium, comprising the Regional Universities Forum for Capacity Building in Agriculture (RUFORUM), the West African Science Service Centre on Climate Change and Adapted Land Use (WASCAL), and AKADEMIYA2063 [International Development Research Centre (IDRC) — No. 109705-001/002] (by SO), the Institut de Recherche pour le Développement (IRD), France (UMR IGE Imputation 252RA5 by AD), and the Agence Nationale de la Recherche (ANR Grant Number 400914/00 by AD). The funders had no role in study design, data collection and analysis, decision to publish, or preparation of the manuscript.

Competing interests: The authors have declared that no competing interests exist.

such as enhancing hydropower system resilience, diversifying energy portfolios, and integrating renewable sources to mitigate climate risks. Hydropower managers and policymakers must prioritize proactive measures to ensure energy security and sustainable resource management amid changing climatic conditions.

1 Introduction

The urgent need to accelerate the transition to renewable energy while phasing out fossil fuels was a central theme at the 29th Conference of the Parties (COP29), held in Baku (Azerbaijan) from November 11–12, 2024. Achieving Net Zero carbon emission requires tripling the share of renewable energy in the global energy mix and scaling up installed capacity from 3.8 TW in 2022 to 11.2 TW by 2030. Among renewable energy sources, hydropower (HP) is recognized as a key option due to its low carbon emissions [1]. HP is currently the largest source of renewable energy, contributing approximately 16% of the world's electricity production [2]. Thus, efforts to mitigate climate change are increasingly emphasizing the role of hydropower on a global scale. As a result, the global installed HP capacity has grown from 1,308 GW in 2019 [2] to 1,416 GW in 2023 [1], an increase of 8.26%.

In Africa, the installed HP capacity has grown even faster, rising from 35 GW in 2019 [2] to 42 GW in 2023 [1], an increase of 13.5%. Despite these promising developments, energy demand in Africa is growing twice as fast as the global average [1]. In addition, HP is increasingly threatened by the effects of climate change [3]. In regions such as West Africa (WA), where HP plays a crucial role in electricity production, these climate-related changes could intensify energy insecurity and contribute to greater economic instability.

The sustainability of hydropower plants relies on the water availability in reservoirs or rivers, which is highly dependent on climate variables, primarily precipitation and temperature [4]. Numerous studies have consistently shown rising temperatures across WA, with warming intensity varying by region [5,6]. Precipitation patterns are expected to be uncertain across WA, with increases in some areas and decreases in others [5–7]. As global warming progresses, HP generation will become more sensitive to fluctuations in weather and climate conditions [4]. Projections are expected to vary at both the national and HP plant-specific levels [7,8]. In such a context, the capacity to reliably quantify these spatially differentiated impacts is not merely an academic exercise, it is a prerequisite for climate-resilient energy infrastructure planning and adaptive water governance across the region.

Recent studies have highlighted the effectiveness of Machine Learning (ML) models in assessing the impacts of climate change on the inflow to reservoirs and energy at HP Plants (HPPs), based on climate variables. In this context, [9] applied an Artificial Neural Network (ANN) to simulate future runoff and hydropower potential in the Hanseok small hydropower plant (South Korea) by 2030, based on the Representative Concentration Pathway (RCP) 4.5 scenario from the HadGEM3-RA (CMIP5) model. [10] employed a Random Forest model to project streamflow in the Konya Closed basin (Turkey) under two Shared Socioeconomic Pathways (SSP2-4.5

and SSP5-8.5), using outputs from five CMIP6 models by 2075. In WA, [7] developed a two-step Random Forest model to project inflow to the Faye HPP (Côte d'Ivoire) by 2100 using thirteen CMIP6 models and their EnsMean. Similarly, [3] proposed a three-step Random Forest model to simulate inflow and energy at the Buyo, Kossou, and Taabo HPPs by 2100, using the EnsMean of eleven models from Coordinated Regional Downscaling Experiment (CORDEX) Africa. Additionally, [11] proposed three-step ensemble ML to simulate inflow and energy at the Nangbeto HPP (Togo) by 2100 using the EnsMean of eleven models from CORDEX-Africa. They considered eight algorithms for the first step.

Despite these advances, several methodological and scientific gaps persist. While these studies employed advanced ML techniques, they share certain limitations. Most analyses have been conducted at local or regional scales, focusing on one or a limited number of ML algorithms. This narrow algorithm selection limits the exploration of alternative methods for improving predictive accuracy and the ability to identify the most suitable learners for HPP-specific hydroclimatic dynamics. In addition, the studies often rely on the EnsMean outputs from climate models without assessing the uncertainty associated with individual model projections, thereby masking the range of plausible future hydroclimatic conditions. Furthermore, previous studies in WA have generally examined only one or a few hydropower systems at a time, limiting the regional understanding of how climate impacts may spatially differ across major hydropower basins. Existing frameworks have also primarily relied on simpler two-step or three-step ML structures, which may not fully optimize model selection, ensemble refinement, and predictor reduction. Taken together, these limitations reduce the robustness and transferability of existing impact assessments and constrain their utility for regional energy planning.

This study addresses these scientific gaps through three main innovations. First, we develop a progressive five-layer ensemble ML framework that improves predictive performance through iterative algorithm screening, ensemble stacking, weak learner elimination, and predictor optimization. This design explicitly targets the bias-variance trade-off by combining strong, diverse learners and progressively removing those that contribute noise rather than complementary predictive information. Second, we assess climate change impacts simultaneously across seven HPP basins in WA, offering a broader regional perspective compared with prior site-specific studies. This multi-basin design enables the identification of spatial contrasts in hydropower vulnerability that would remain invisible in single-site analyses. Third, instead of relying solely on climate EnsMean, the study accounts for uncertainty across individual climate model projections, thereby improving confidence in future inflow and energy assessments.

The originality of this work therefore lies not only in methodological advancement but also in its regional-scale application and uncertainty-aware design. These contributions improve methodological rigor and provide more reliable evidence for HP vulnerability assessment, supporting climate-resilient electricity planning and adaptive water resource governance in a region where energy demand is rapidly increasing under climate stress.

The study begins with an overview providing context and objectives, followed by a detailed description of the data and methodologies employed. Next, the key findings are presented, emphasizing model performance, statistical analyses, and projected changes for both near and far futures. This is followed by a discussion interpreting the results. Finally, the concluding section summarizes the main insights and highlights key findings.

2 Data and methods

This study focuses on seven HP dam basins across WA (Fig 1): (1) the Manantali HP dam basin drained by the Bafing River, the main tributary of the Senegal River. It is a transboundary basin shared between Mali and Guinea. (2) The Buyo and (3) Taabo HP dam basins, both located in Côte d'Ivoire and drained by the Sassandra and Bandama Rivers, respectively. (4) The Akosombo, (5) Kpong and (6) Bagre HP dam basins drained by the Volta River. The Volta River is a transboundary River shared between Benin, Burkina Faso, Côte d'Ivoire, Ghana, Mali and Togo [12]. Both Akosombo and Kpong dams are located in Ghana, but have a transboundary basin shared between the six countries cited above. The Bagre dam basin is located in Burkina Faso. (7) The Nangbeto HP basin drained by the Mono River. It is a transboundary basin shared between Togo and Benin. The basin areas are around 403,612 km^2 for Kpong,

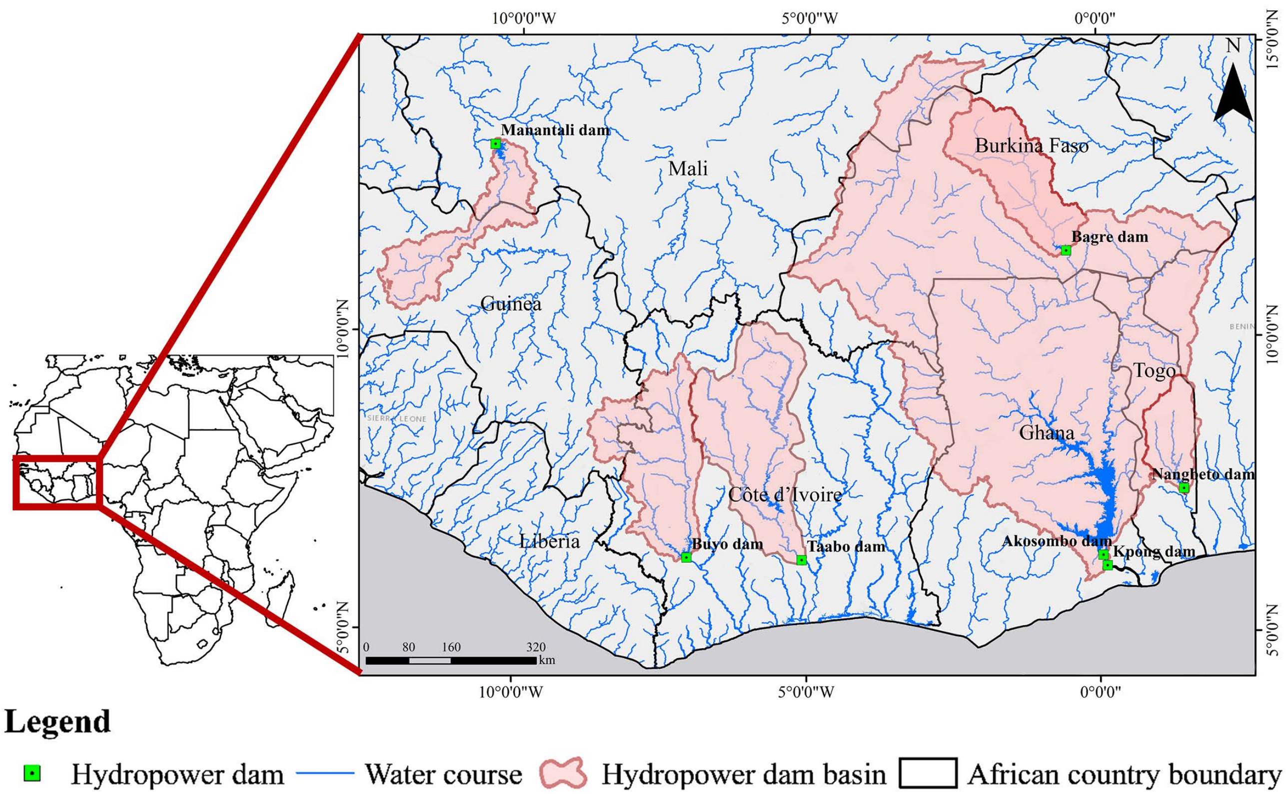

Fig 1. Study area. Country boundaries and river network from Natural Erath (Public domain); Basin boundaries derived from United States Geological Survey (USGS) Digital Elevation Model (DEM) data (Public domain).

https://doi.org/10.1371/journal.pclm.0000986.g001

403,007 km^2 for Akosombo, 61,512 km^2 for Taabo, 47,861 km^2 for Buyo, 35,347 km^2 for Bagre, 28,615 km^2 for Manantali and 16,688 km^2 for Nangbeto. The installed capacity of these dams is 1,020 MW and 160 MW for Akosombo and Kpong, respectively [12], 210 MW and 165 MW for Taabo and Buyo, respectively [13], 16 MW for Bagre [14], 65 MW for Nangbeto [15], and 200 MW for Manantali [16].

2.1 Data

The data used in this study are subdivided into two groups: (1) climate data and (2) inflow and energy data.

2.1.1 Climate data. In this study, the CHIRPS (Climate Hazard Infrared Precipitation with Station) data for precipitation and CHIRTS (Climate Hazard Infrared Temperature with Station) data for average temperature were used as observational datasets. These datasets, with a spatial resolution of 0.05° (approximately 5 km), are freely available via https://data.chc.ucsb.edu/products/CHIRPS-2.0/ for CHIRPS and via https://data.chc.ucsb.edu/products/CHIRTSdaily/ for CHIRTS. These datasets were utilized at a monthly scale for the period from 1983 to 2016. The selection of these datasets was based on their demonstrated accuracy in estimating monthly climate observations over WA [7,17–19].

For climate projections, precipitation and average temperature data from the outputs of twelve CMIP6 models (Table 1) were considered under the SSP1-2.6, SSP2-4.5, and SSP5-8.5 scenarios. The CMIP6 model outputs are freely accessible via the Earth System Grid Federation (ESGF) portal https://esgf-node.ipsl.upmc.fr/search/cmip6-ipsl/. The historical period covered 1983–2014, while projections spanned 2036–2099. These models have been widely used in global studies [20–23] and have shown strong performance in simulations over the Faye HP dam basin (Côte d'Ivoire, WA) in the study by [7]. The EnsMean of these projections was employed for analysis.

Table 1. CMIP6 GCM used in this study.

Model	Institution	Spatial resolution (lon × lat)
CanESM5	Canadian Center for Climate Modeling and Analysis (CCCma)	2.8125° × ~2.7673°
CESM2-WACCM	National Center for Atmospheric Research (NCAR)	1.25° × 0.9°
CMCC-ESM2	Euro-Mediterranean Center on Climate Change (CMCC)	1.25° × 0.9°
FGOALSg3	Chinese Academy of Sciences, Flexible Global Ocean-Atmosphere-Land System Model	2° × 2°
IITM-ESM	Indian Institute for Tropical Meteorology (IITM)	1.875° × 1.914°
INM-CM4–8	Institute for Numerical Mathematics	2° × 1.5°
IPSL-CM6A-LR	Pierre Simon Laplace Institute (IPSL)	2.5° × 1.27°
MIROC6	Japan Agency for Marine-Earth Science and Technology (JAMSTEC)	1.40625° × ~1.39°
MPI-ESM1–2-LR	Max Planck Meteorological Institute (MPI)	1.875° × 1.85°
MRI-ESM2–0	Meteorological Research Institute (MRI)	1.125° × ~1.11°
NESM3	University of Science and Technology of Nanjing	1.875° × ~1.7°
NorESM2-LM	Norvegian Climate Center	2.5° × 1.9°

https://doi.org/10.1371/journal.pclm.0000986.t001

2.1.2 Inflow and energy data. Monthly inflow data to four HPPs (Buyo, Manantali, Nangbeto, and Taabo) were collected up to 2016. Additionally, monthly energy data from six HPPs (Akosombo, Bagre, Buyo, Kpong, Nangbeto, and Taabo) were also compiled for the same period. Notably, there was no missing data in the inflow and energy time series, except for the energy data from the Nangbeto HPP, which had a 2% data gap in 1987. A summary of the collected data is provided in Table 2. These data were collected from national structures in charge of energy production.

2.2 Methods

2.2.1 Bias adjustment. Before using projections data, the precipitation and average temperature data from the twelve CMIP6 climate models were bias-adjusted using the delta change approach. This approach effectively adjusts the mean, variance, and probability density function of the model outputs to align with the observed data [24]. Specifically, for precipitation, multiplicative delta factors were applied to preserve the relative change signal, while additive delta factors were used for temperature to capture shifts. This distinction ensures physically consistent adjustments across both variables. This method is straightforward to implement, and has proven effective at the Fayé HP dam basin and monthly scales [7].

2.2.2 Model development. This study presents a progressive five-layer ensemble modeling framework designed to iteratively improve prediction accuracy, reduce model uncertainty, and optimize predictor selection across seven HP dam basins in WA. The rationale for using five successive layers is to gradually refine the modeling structure: first by identifying strong individual learners, then by combining them into ensembles, next by eliminating weak contributors, and finally by testing predictor completeness versus predictor reduction. This hierarchical strategy ensures that both algorithm selection and predictors selection are systematically optimized rather than addressed in a single step. In this framework, numerous base learners are trained as an ensemble to combine model predictions into a single output that outperforms individual ensemble members by minimizing uncorrelated errors on the target datasets.

The theoretical foundation of this framework is rooted in ensemble learning theory and the bias-variance trade-off. Ensemble methods combine multiple models to improve predictive performance by reducing variance and/or bias while enhancing generalization capability. Recent studies confirm that ensemble approaches, such as bagging, boosting, and stacking, consistently outperform single models across a wide range of applications due to their ability to capture

Table 2. Brief description of target variables.

Hydropower plant	Period	Missing values (%)
Inflow		
Buyo	1983-2016	0
Manantali	1983-2016	0
Nangbeto	1987-2016	0
Taabo	1983-2016	0
Energy		
Akosombo	1983-2016	0
Bagre	2009-2016	0
Buyo	1983-2016	0
Kpong	1984-2016	0
Nangbeto	1987-2016	2
Taabo	1983-2016	0

https://doi.org/10.1371/journal.pclm.0000986.t002

complementary patterns and reduce prediction errors [25]. In particular, stacking-based frameworks have been shown to provide superior predictive accuracy by integrating heterogeneous learners into a unified model structure [26].The model ensemble mean was developed using the *caretStack* function from the *caretEnsemble* package in R, which integrates multiple predictive models through stacking [11]. This process was conducted across five layers, each designed to refine model performance progressively. The k-fold cross validation was used with $k = 10$, selected because preliminary testing showed that this configuration provided the best balance between predictive accuracy and model stability.

For the first layer, fifteen algorithms, as detailed in Table 3, were applied to the two target variables (Fig 2). This initial screening phase aimed to establish a broad benchmark of candidate models with diverse learning structures. Model performance was evaluated using cross-validated predictive metrics, and algorithms were ranked according to their overall predictive skill. The five lowest-performing algorithms were excluded, specifically those consistently showing higher prediction errors and lower explained variance relative to competing models. This exclusion criterion was applied

Table 3. Algorithms used in this study.

Algorithm	Abbreviation
Bagged CART (Classification And Regression Tree)	treebag
Boosted Generalized Linear Model	glmboost
Boosted Tree	blackboost
CART	rpart2
Conditional Inference Random Forest	cforest
Conditional Inference Tree	ctree
Independent Component Regression	icr
k-Nearest Neighbors	knn
Lasso and Elastic-Net Regularized Generalized Linear Models	glmnet
Linear Regression	lm
Quantile Random Forest	qrf
Random Forest	rf
Stochastic Gradient Boosting	gbm
Support Vector Machines with Polynomial Kernel	svmPoly
Support Vector Machines with Radial Basis Function Kernel	svmRadial

https://doi.org/10.1371/journal.pclm.0000986.t003

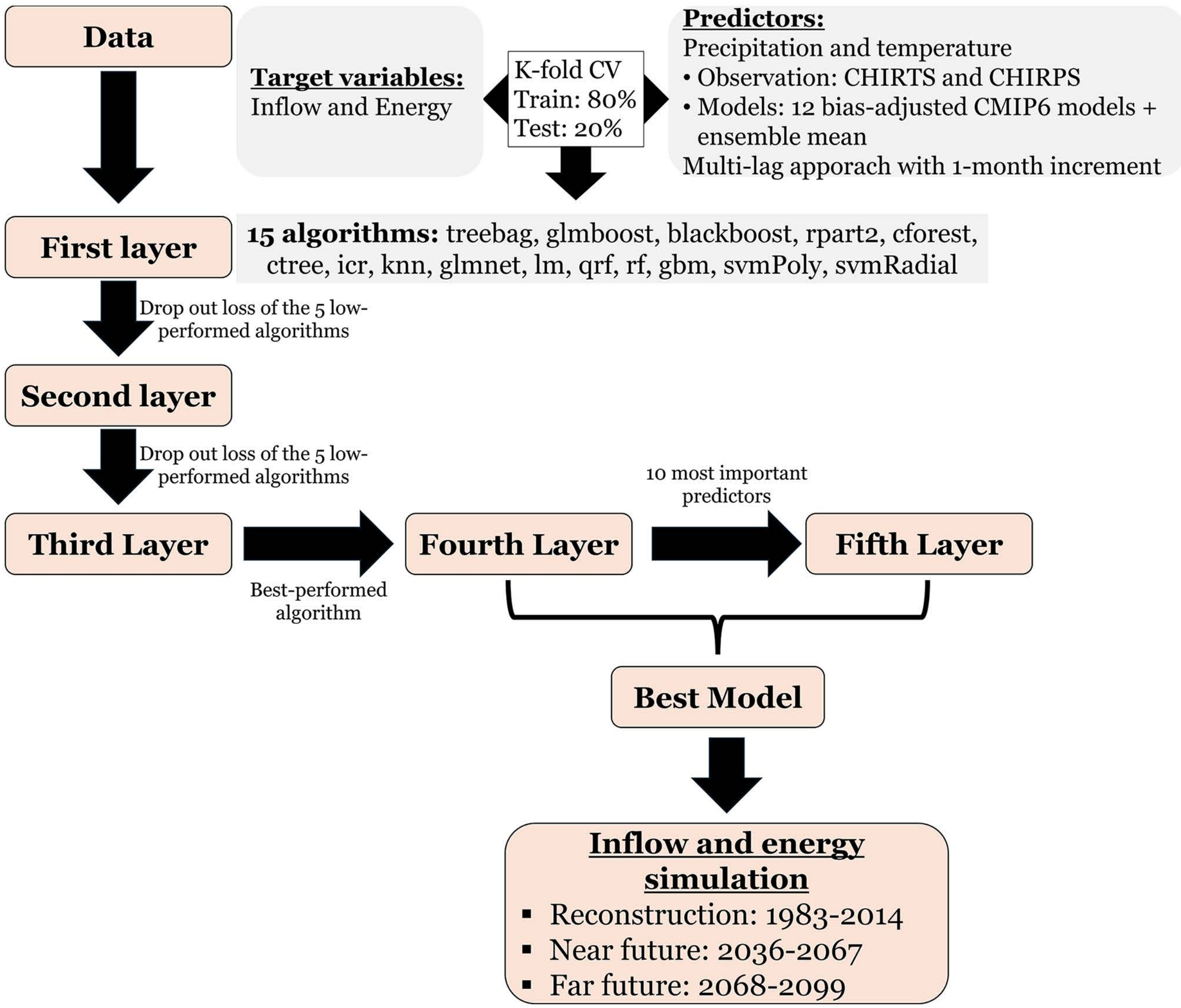

Fig 2. Flowchart of the model development.

https://doi.org/10.1371/journal.pclm.0000986.g002

to remove weak learners likely to contribute noise rather than complementary predictive information to the ensemble. The second layer was constructed by creating an ensemble mean using the top 10 performing algorithms for each target variable. The purpose of this layer was to exploit ensemble learning benefits by combining strong but diverse models, thereby reducing individual model bias and variance. The third layer further refined the ensemble by again excluding the five lowest-performing algorithms, leaving only the top-performing models to build the ensemble mean. This second filtering stage was necessary to retain only the most robust contributors after ensemble interaction effects were observed, ensuring that poorly complementary models did not dilute ensemble efficiency.

The fourth layer utilized the best-performing ensemble from the previous layers, but incorporated all predictors, including precipitation, temperature, and lagged values, to assess overall predictive capacity. This layer served as a full-information benchmark to evaluate the maximum predictive potential when no dimensionality reduction is imposed.

Finally, the fifth layer focused on optimizing model efficiency by using only the 10 most important predictors as identified by the best-performing algorithm. [7] demonstrated that reducing the number of predictors can enhance model performance. Their study, which employed Random Forest over the Fayé HP dam basin, underscores the importance of dimensionality reduction in improving predictive accuracy. Accordingly, this fifth layer tested whether predictor reduction could maintain or improve predictive skill while reducing redundancy, overfitting risk, and computational complexity. The final model was developed by selecting the best model from these two approaches: (1) all predictors with the best-performing algorithms in the fourth layer, and (2) the ten most important predictors with the best-performing algorithms in the fifth layer. The selected final configuration was the one achieving the best trade-off between predictive performance, robustness, and model simplicity. To assess whether projected future distributions of inflow and energy differ significantly from the reference period, the non-parametric Wilcoxon signed-rank test was applied at a 95% confidence level. The methodology used in the present study is synthesized in the following flowchart (Fig 2).

2.2.3 Predictors. Precipitation and temperature were selected as the key climate predictors for this study. For the historical period, precipitation and temperature data were sourced from CHIRPS and CHIRTS, respectively. For projections, precipitation and temperature data from twelve CMIP6 climate model outputs and their EnsMean under the SSP1-2.6, SSP2-4.5 and SSP5-8.5 scenarios were considered. Indeed, climate variables (precipitation and temperature) have shown their reliability for modeling inflow and energy [27,28]. Moreover, the multi-lag approach was applied in the present study. This approach has shown its efficiency for modeling inflow and energy [27]. Thus, precipitation and temperature data were lagged up to twelve and six months, respectively, with a one-month increment [7,11].

2.2.4 Model performance evaluation. The performance of models for each layer was assessed using four indicators (1) the coefficient of determination (R^2), (2) the Nash-Sutcliffe model Efficiency coefficient (NSE), (3) the Mean Absolute Percentage Error (MAPE), and (4) the percentage Root Mean Square Error (RMSE). These indicators have been utilized in numerous studies, with further details available [29–31].

3 Results

3.1 Evaluation of the five-layer model

The target variables (inflow and energy) were simulated using an ensemble learning approach comprising fifteen ML algorithms, with the five lowest-performing algorithms excluded in the first two layers. The results revealed a reduction in computational time with the exclusion of five low-performing algorithms. For inflow to HPP (Fig 3), all algorithms showed good performance regardless of the layer and HPP, with $R^2 > 0.6$, NSE > 0.6, and MAPE < 0.2. RMSE < 0.5 was recorded for inflow to the Buyo and Manantali HPPs, while RMSE ≥ 0.5 was recorded for inflow to the Nangbeto and Taabo HPPs. The higher RMSE values at Nangbeto and Taabo suggest greater absolute prediction errors at these HPPs, likely reflecting the more complex or variable hydrological regimes of their upstream catchments. Despite this, the consistently high R^2 and NSE values confirm that the algorithms captured the dominant temporal dynamics of inflow across all HPPs, indicating strong predictive skill.

In the second layer, the two HPPs of Côte d'Ivoire (Buyo and Taabo) exhibited the same top ten algorithms, namely blackboost, cforest, gbm, glmnet, knn, qrf, rf, svmPloy, svmRadial, and treebag. The Manantali and Nangbeto HPPs shared nine of these algorithms (9/10, or 90%) with Buyo and Taabo. The high degree of overlap in top-performing algorithms across geographically distinct HPPs, located in different countries and river basins, suggests that ensemble-based tree methods (e.g., rf, cforest, gbm) and kernel-based approaches (e.g., svmPoly, svmRadial) are broadly suited to modeling inflow dynamics in West African hydrological contexts. The minor differences in algorithm selection between HPPs may reflect subtle differences in the statistical structure of local inflow time series, such as distributional skewness or the degree of nonlinearity in rainfall-runoff relationships.

In the third layer, both Nangbeto and Taabo HPPs exhibited the same five best-performing algorithms: cforest, qrf, rf, svmPoly, and svmRadial. The Manantali HPP shared four of these top algorithms (4/5, or 80%) with Nangbeto and Taabo. For Buyo, three best-performing algorithms (3/5, or 60%) were shared with Manantali, and four of the top five algorithms (4/5, or 80%) were shared with Nangbeto and Taabo. The persistence of svmPoly and svmRadial among

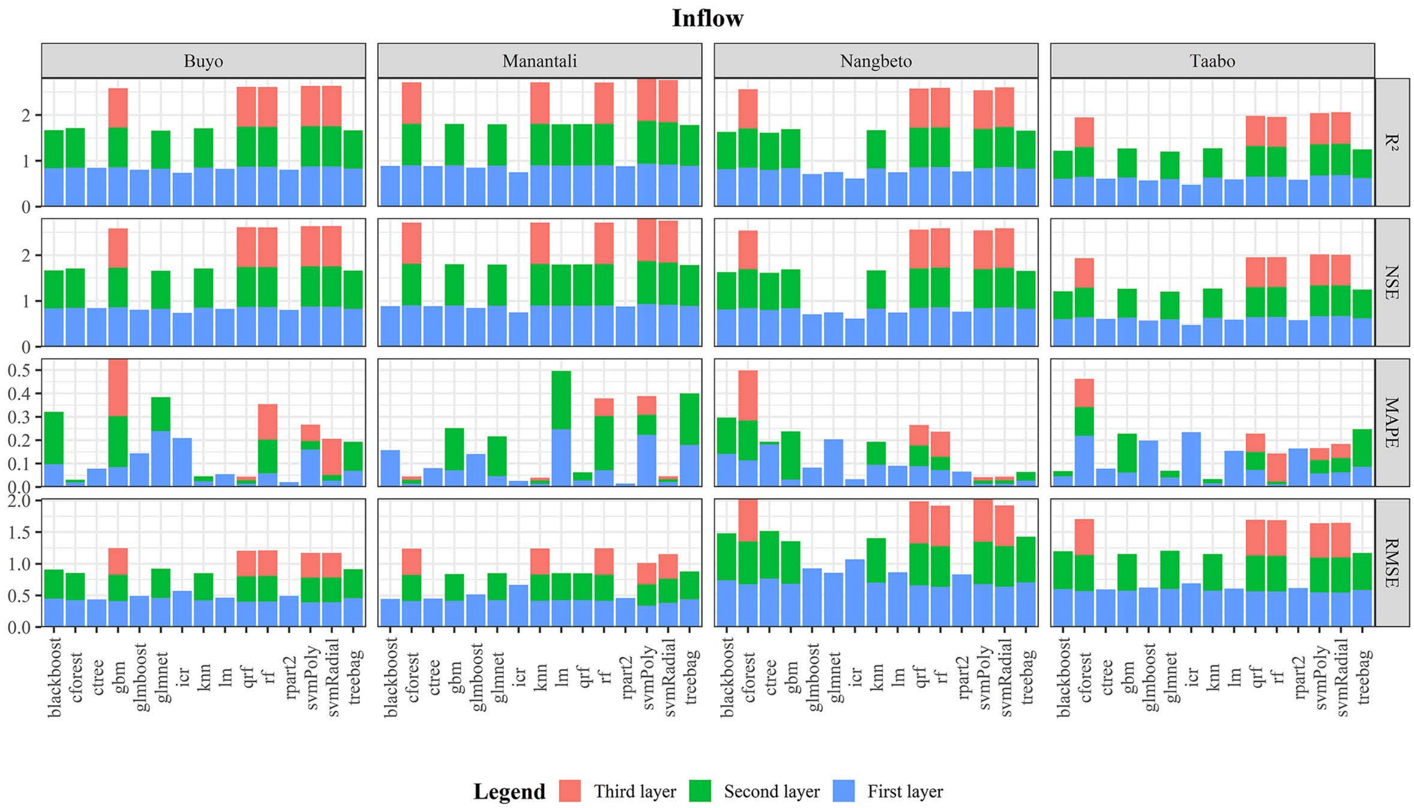

Fig 3. Metrics performance of algorithms in ensemble learning for inflow to HPP (m^3/s). (a) First layer. (b) Second layer. (c) Third layer.

https://doi.org/10.1371/journal.pclm.0000986.g003

the top algorithms across layers and HPPs underscores the robustness of support vector machine-based methods for inflow prediction. This is likely due to their capacity to handle nonlinear predictor-response relationships through kernel transformation and their inherent regularization properties that penalize model complexity and reduce overfitting risk in high-dimensional lagged predictor spaces. The presence of ensemble tree-based methods (rf, cforest, qrf) alongside svm algorithms further suggests that both flexible nonparametric and margin-based approaches are complementary in capturing the hydrological signal. The slightly lower algorithm overlaps at Buyo compared to the other HPPs may be attributable to the unique catchment characteristics of the Sassandra River basin.

For energy by HPP (Fig 4), the results showed poor performance of algorithms for Akosombo, Bagre, Buyo, Kpong, and Taabo, with $R^2 < 0.6$ and NSE < 0.6, regardless of the algorithm, layer, and HPP. The MAPE and RMSE were lower than 0.5. In contrast, for the Nangbeto HPP, all the algorithms exhibited good performance, achieving $R^2 > 0.6$, NSE > 0.6, MAPE < 0.2, and RMSE < 0.5. An exception was recorded for the icr algorithm, which showed R^2 and NSE lower than 0.5, and RMSE exceeding 0.5. The poor performance of icr at Nangbeto, in contrast to all other algorithms, suggests that this method is less well-suited to capturing the nonlinear dynamics of energy generation at this HPP, and further justifies its exclusion in subsequent layers.

In the second layer, no HPPs displayed identical sets of top ten performing algorithms. The Bagre and Buyo HPPs shared nine algorithms (9/10, or 90%), namely cforest, gbm, glmboost, glmnet, lm, rf, svmPoly, svmRadial, and treebag. The four other HPPs (Akosombo, Kpong, Nangbeto, and Taabo) shared six algorithms (6/10, or 60%), specifically blackboost, cforest, qrf, rf, svmPoly, and treebag. The Akosombo and Kpong HPPs, both located in Ghana, exhibited the greatest similarity, sharing an additional three algorithms (ctree, glmnet, and rpart2), totaling nine algorithms in common.

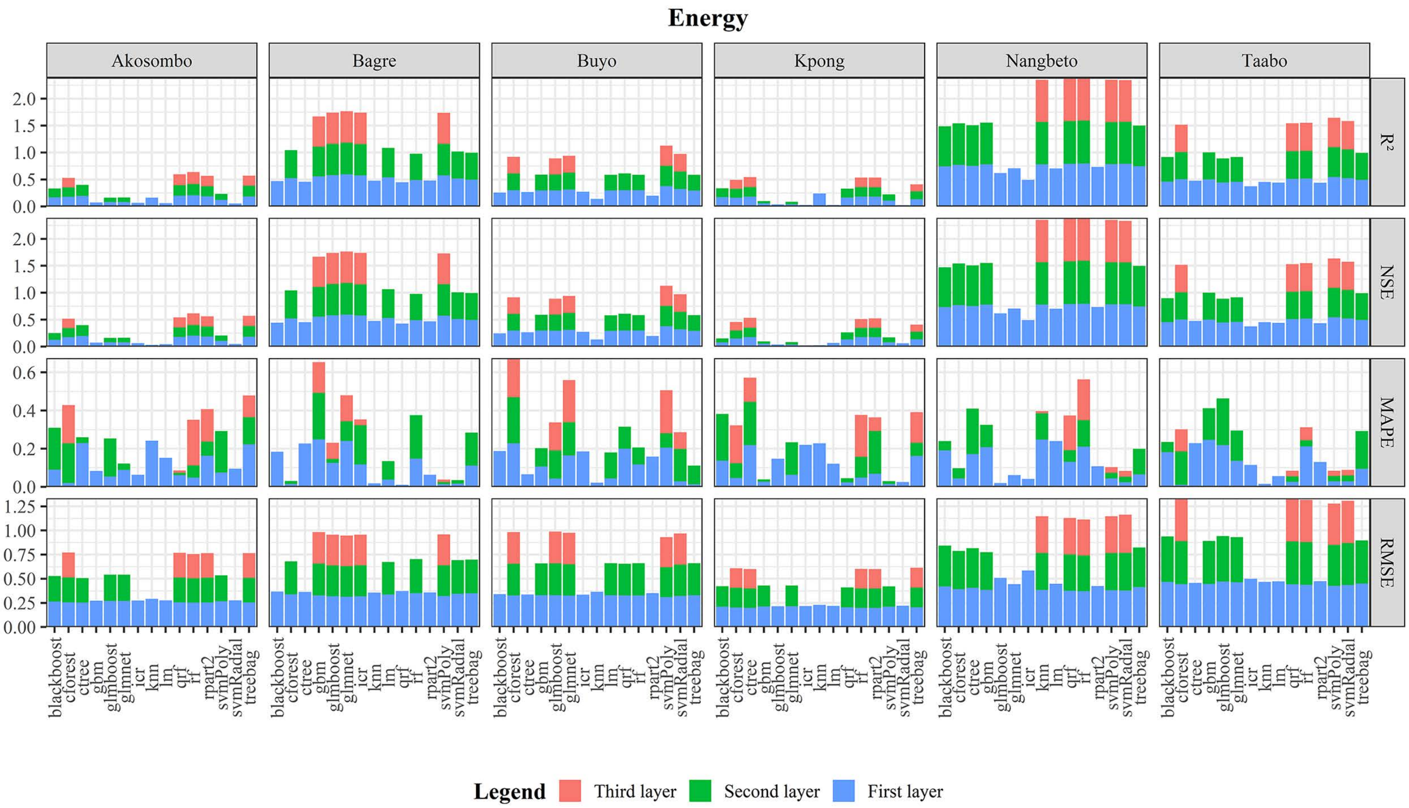

Fig 4. Performance metrics of algorithms in ensemble learning for energy by HPP (MW). (a) First layer. (b) Second layer. (c) Third layer.

https://doi.org/10.1371/journal.pclm.0000986.g004

In the third layer, no HPPs displayed identical sets of top-performing algorithms. However, Akosombo and Kpong again recorded the greatest similarity, with four algorithms shared out of five (4/5, or 80%): cforest, qrf, rpart2, and treebag. The Taabo HPP shared two algorithms (cforest and rf) in common with Akosombo and Kpong, while Buyo shared only one algorithm (cforest) with the other HPPs.

For the fourth layer, the best-performing algorithm was selected for each target variable and HPP (Table 4). Regarding inflow to reservoirs, the svm algorithm group demonstrated outperformance across all analyzed HPPs. Specifically, svmRadial showed the best performance for inflows to Buyo and Nangbeto (2/4, approximately 50%), while svmPoly performed best for Manantali and Taabo (2/4, approximately 50%). In these cases, the R^2 and NSE values exceeded 0.7, while MAPE remained below 0.06. The RMSE was less than 0.4 for inflows to Buyo and Manantali but exceeded 0.5 for Nangbeto and Taabo. Notably, for inflow to Taabo, selecting the single best-performing algorithm significantly improved performance. While the first three layers exhibited low performance for this HPP, the independent application of the best-performing algorithm produced satisfactory results ($R^2 > 0.6$, NSE > 0.6, MAPE < 0.1, and RMSE < 0.5).

For energy predictions, the results were more varied. The best-performing algorithms were rf for Akosombo and Nangbeto (2/6, or 33%), svmPoly for the two HPPs in Côte d'Ivoire (Buyo and Taabo; 2/6, or 33%), glmboost for Bagre (1/6, or 17%), and ctree for Kpong (1/6, or 17%). Selecting the best-performing algorithm enhanced performance for the Bagre, Buyo, and Taabo HPPs. In these cases, algorithms that had underperformed in the previous layers exhibited improved performance when applied individually, achieving $R^2 > 0.5$, NSE > 0.5, and lower MAPE and RMSE values. The

Table 4. Best-performing algorithm for inflow and Energy.

HPP	Best Algorithm	R^2	NSE	MAPE	RMSE
Inflow					
Buyo	svmRadial	0.9	0.9	0.007	0.35
Manantali	svmPoly	0.95	0.95	0.002	0.28
Nangbeto	svmRadial	0.9	0.89	0.01	0.54
Taabo	svmPoly	0.71	0.71	0.054	0.52
Energy					
Akosombo	rf	0.22	0.21	0.1	0.25
Bagre	glmboost	0.63	0.63	0.043	0.29
Buyo	svmPoly	0.51	0.5	0.01	0.27
Kpong	ctree	0.2	0.2	0.2	0.2
Nangbeto	rf	0.8	0.8	0.007	0.37
Taabo	svmPoly	0.65	0.65	0.032	0.37

https://doi.org/10.1371/journal.pclm.0000986.t004

heterogeneity of best-performing energy algorithms across HPPs, spanning tree-based, kernel-based, and linear boosting methods, reflects the diversity of energy generation regimes across the study sites and reinforces the importance of site-specific algorithm evaluation rather than assuming transferability of optimal models across basins.

For inflow (Fig 5a), selecting the ten most important predictors slightly improved the performance of svmRadial for the Buyo and Nangbeto HPPs. In contrast, it reduced the performance of svmPoly for Manantali and Taabo HPPs. Thus, reducing the number of predictors enhanced the performance of svmRadial, but was ineffective for svmPoly, leading to a decline in its performance.

For energy (Fig 5b), the performance of the best-performing algorithm remained low for the Akosombo, Buyo and Kpong HPPs. However, developing models based on the single best-performing algorithm improved performance for Bagre, Buyo, and Taabo, compared to the first three layers. Selecting the ten most important predictors improved the performance of glmboost for Bagre and ctree for Kpong. However, as observed in inflow, reducing the predictors negatively impacted the performance of svmPoly for the Buyo and Taabo HPPs. This asymmetric response to predictor reduction suggests that svmRadial, with its radial basis function kernel, is more sensitive to redundant or noisy predictors. However, svmPoly, operating in a polynomial feature space, benefits from the full predictor set to construct more complex decision boundaries. For rf, the reduction in predictors had no significant effect on algorithm performance. These findings highlight that optimal predictor dimensionality is algorithm-dependent and cannot be determined a priori without testing.

Overall, the five-layer framework demonstrated that a hierarchical ensemble strategy can effectively identify HPP-specific optimal algorithms for inflow and energy prediction. The svm family consistently excelled for inflow simulation, while a more heterogeneous set of algorithms was required for energy. This is a distinction that reflects the greater complexity and operational dependency of energy generation compared to inflow, which is more directly driven by climatic forcing.

3.2 Evolution of precipitation and temperature

Temperature and precipitation changes were analyzed using twelve climate models and their EnsMean under SSP1-2.6, SSP2-4.5, and SSP5-8.5 for the near (2036–2067) and far (2068–2099) future, relative to the 1983–2014 reference period. Results (Fig 6 and S1 to S7 Fig) indicate unanimous model agreement on warming, with EnsMean projecting temperature (temp) increases of up to 4.5°C and individual models predicting localized warming up to 7°C. Warming intensity varies across basins and is more pronounced in the far future. Among the scenarios, SSP5-8.5 projects the highest temperature rise, surpassing SSP2-4.5 and SSP1-2.6.

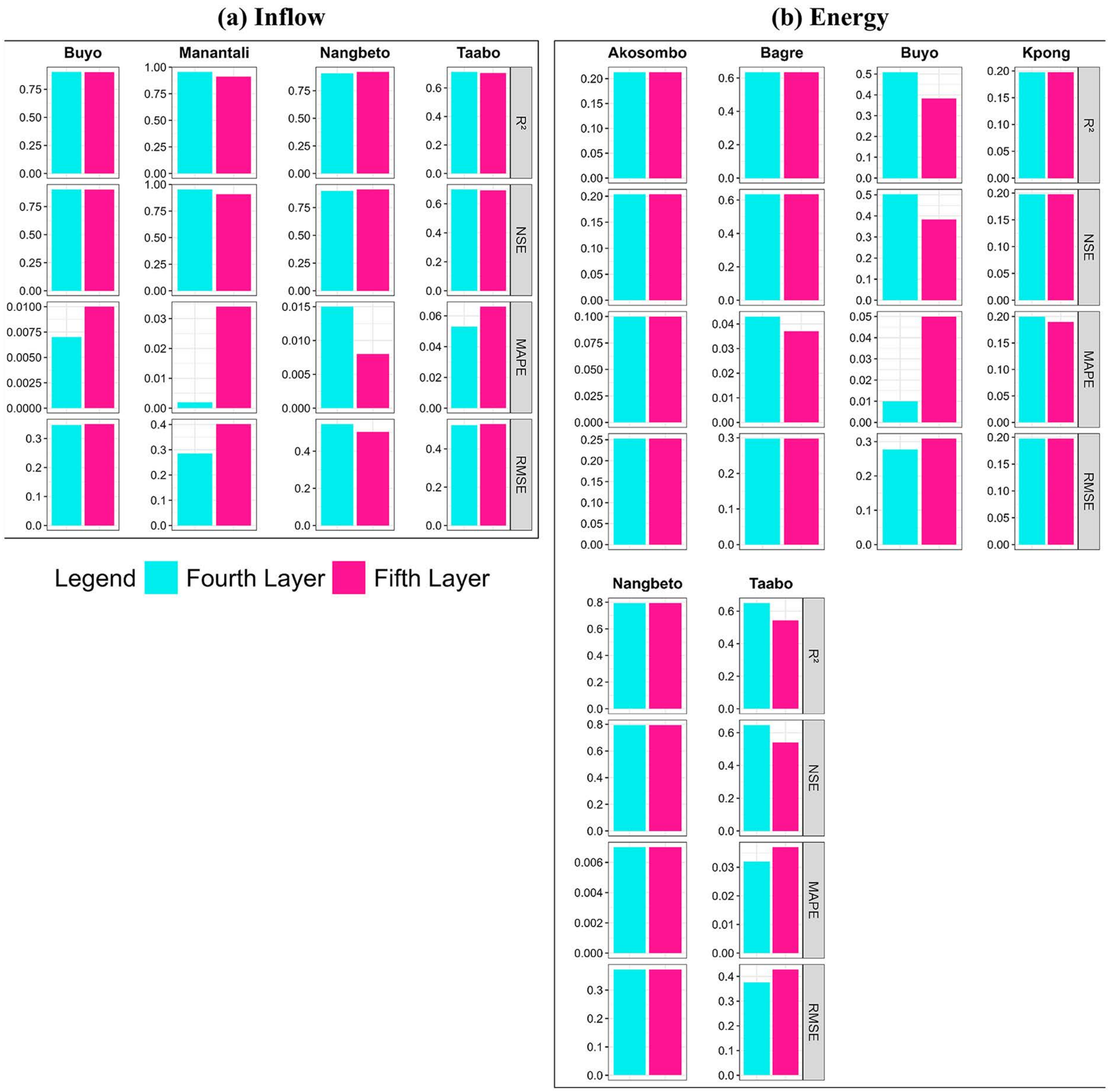

Fig 5. Metric performance of the best-performed algorithm for the fourth and fifth layers. (a) Inflow. (b) Energy.

https://doi.org/10.1371/journal.pclm.0000986.g005

Among the analyzed models, MPI-ESM1–2-LR consistently projected the lowest warming, while CanESM5 and CESM2-WACCM showed variable projections of the highest warming across basins, scenarios, and projection periods. The EnsMean projected an average temperature increase of approximately 1.2°C (near future) and 1.3°C (far future) under SSP1-2.6, and 1.5°C (near future) and 2.0°C (far future) under SSP2-4.5, across all basins except Manantali. Under SSP5-8.5, projected warming intensifies, reaching around 2°C in the near future. Warming is projected to increase further in the far future, with temperature rises of approximately 3.5°C over the Nangbeto (Fig 6f), 4°C over the Akosombo (Fig 6a), Bagre (Fig 6b), Buyo (Fig 6c), Kpong (Fig 6d), and Taabo (Fig 6g) dam basins, and up to 4.5°C over the Manantali dam basin. These results highlight the substantial spatial variability in projected warming, with more pronounced increases under high-emission scenarios.

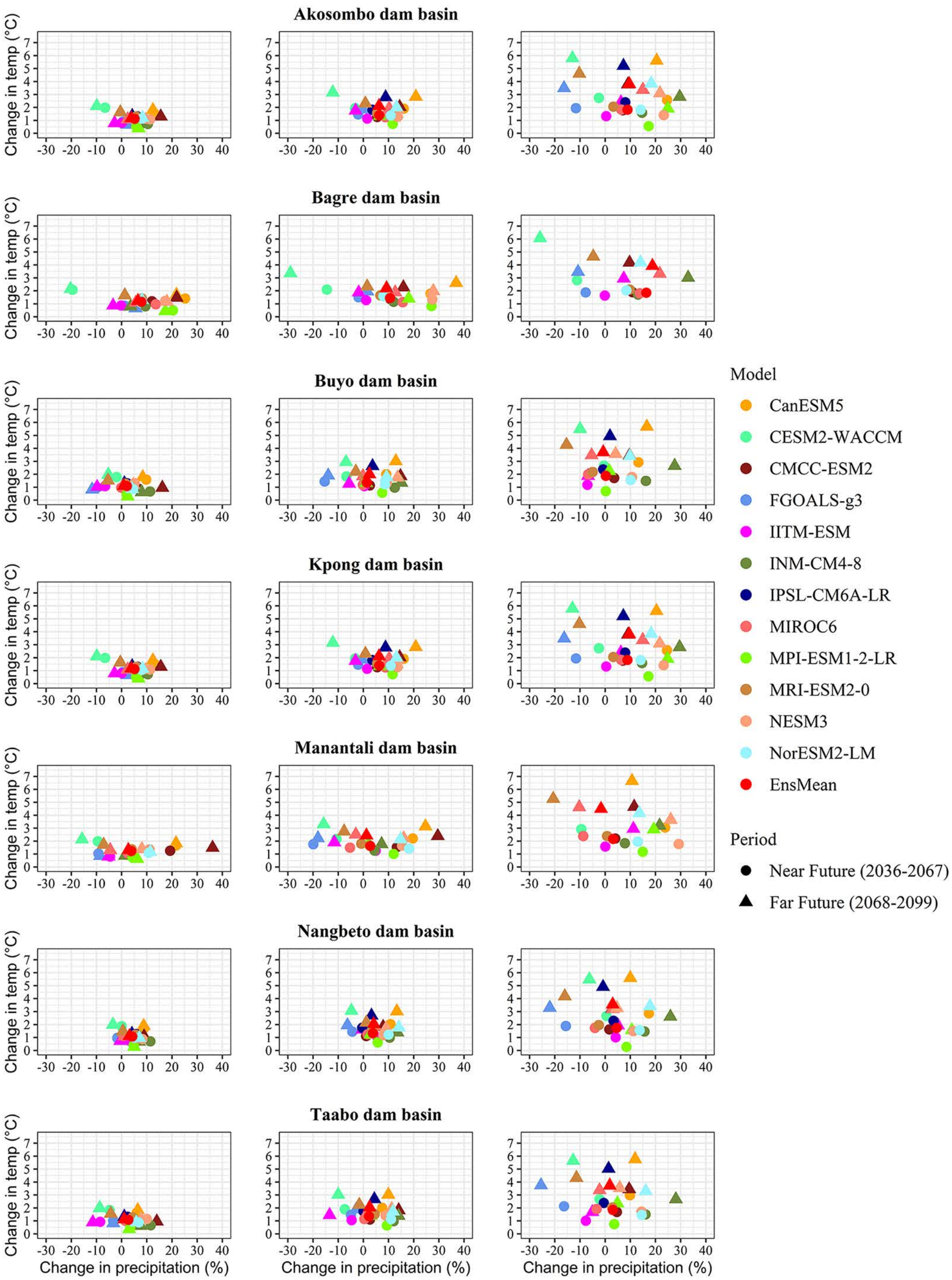

Fig 6. Changes in precipitation and temperature in the near (2036-2067) and far (2068-2099) futures, relative to the reference period (1983-2014). (a) For the Akosombo dam basin. (b) For the Bagre dam basin. (c) For the Buyo dam basin. (d) For the Kpong dam basin. (e) For the Manantali dam basin. (f) For the Nangbeto dam basin. (g) For the Taabo dam basin.

https://doi.org/10.1371/journal.pclm.0000986.g006

Precipitation projections exhibited significant variability across basins, scenarios, and projection periods, with some models predicting decreases of up to 30% and others projecting increases not exceeding 40%. The SSP5-8.5 scenario consistently showed the most pronounced changes, particularly in the far future, compared to SSP2-4.5 and SSP1-2.6. The number of models showing statistically significant differences from the reference period increased progressively from SSP1-2.6 to SSP5-8.5 across all projection periods.

Under SSP1-2.6, CESM2-WACCM projected the largest precipitation decreases for multiple dam basins (Akosombo, Bagre, Kpong and Manantali), while CanESM5 and CMCC-ESM2 showed the highest increases. Similar trends were observed under SSP2-4.5, with CanESM5 consistently predicting the largest precipitation increases for Akosombo and Kpong dam basins. The SSP5-8.5 scenario showed more extreme variations, with FGOALS-g3 projecting the largest decreases and INM-CM4–8 the largest increases across multiple basins (Akosombo, Kpong, Nangbeto, and Taabo).

The EnsMean suggests that in the near future, precipitation will be significantly different from the reference period for Akosombo and Kpong under all scenarios and for Bagre under SSP5-8.5. For the far future, significant changes are expected for Akosombo and Kpong under SSP2-4.5 and SSP5-8.5, as well as for Bagre and Manantali under SSP5-8.5. Overall, SSP1-2.6 and SSP2-4.5 projected slight precipitation increases (≤ 5%) for all basins, except for Manantali, where no change is projected in the near future and a slight decrease (around 2%) was projected in the far future. Under SSP5-8.5, projected increases ranged from 5% to 13% in several basins (up to 5% for Nangbeto and Taabo, from 5% to 10% for Akosombo and Kpong, and from 10% to 13% for Bagre), while Manantali and Buyo were expected to experience decreases by up to 6%. Compared to the near future, precipitation decreases were projected for all basins in the far future under SSP1-2.6, while SSP2-4.5 showed a mix of stable, increasing, and decreasing trends depending on the basin.

These findings highlight the considerable uncertainty in future precipitation patterns, emphasizing the need for basin-specific climate adaptation strategies.

3.3 Changes in simulated target variables

The inflow and energy dynamics were simulated for twelve models and EnsMean under the SSP1-2.6, SSP2-4.5, and SSP5-8.5 scenarios using the best-performing algorithm and the most effective configuration between the fourth and fifth layers. Simulations were computed for HPPs with performance metrics of at least $R^2 \geq 0.6$, NSE ≥ 0.6, and results were compared against the reference period. The results (Fig 7 and S8 to S14 Fig) exhibit variability depending on the target variable, HPP, model, projection period, and scenario. However, the boxplot range of observations during the reference period is larger than the boxplot ranges of simulations under scenarios, regardless of the target variable, models, and HPP, highlighting greater variability in inflow and energy during the reference period, compared to projections.

Regarding the EnsMean inflow changes (Fig 7a), increases are projected for Manantali under all scenarios across all projection periods, while the results seem mixed for the other HPPs. In the near future, projected inflows will be significantly different from the reference period for Buyo under SSP5-8.5 and Manantali under all three scenarios. In the far future, significant differences were noted for Buyo and Manantali under both SSP2-4.5 and SSP5-8.5 and Taabo under SSP5-8.5. A slight increase in inflow to the Buyo HPP is projected only under SSP1-2.6 scenario for both the near and far future, peaking at 3% in the near future. For other scenarios, inflow decreases are projected, with a maximum reduction of 24% in the near future under SSP5-8.5 scenario. In the far future, decreases are projected under all scenarios, relative to the near future. The large projected inflow decrease at Buyo under SSP5-8.5 is particularly alarming from an energy security perspective, as the Buyo HPP is a major electricity producer in Côte d'Ivoire. A 24% decline in near-future inflow under high emissions represents a substantial reduction in hydraulic head and reservoir filling, which would directly constrain generation capacity. For the Nangbeto HPP, inflow is projected to increase only under SSP5-8.5 scenario in the far future, reaching 13% on average compared to the reference period. In contrast, other scenarios predict inflow declines, with the largest decline (7%) occurring in the near future under SSP1-2.6 scenario. Relative to the near future, slight decreases are projected in the far future under SSP1-2.6 scenario, while increases are expected under the other scenarios. The

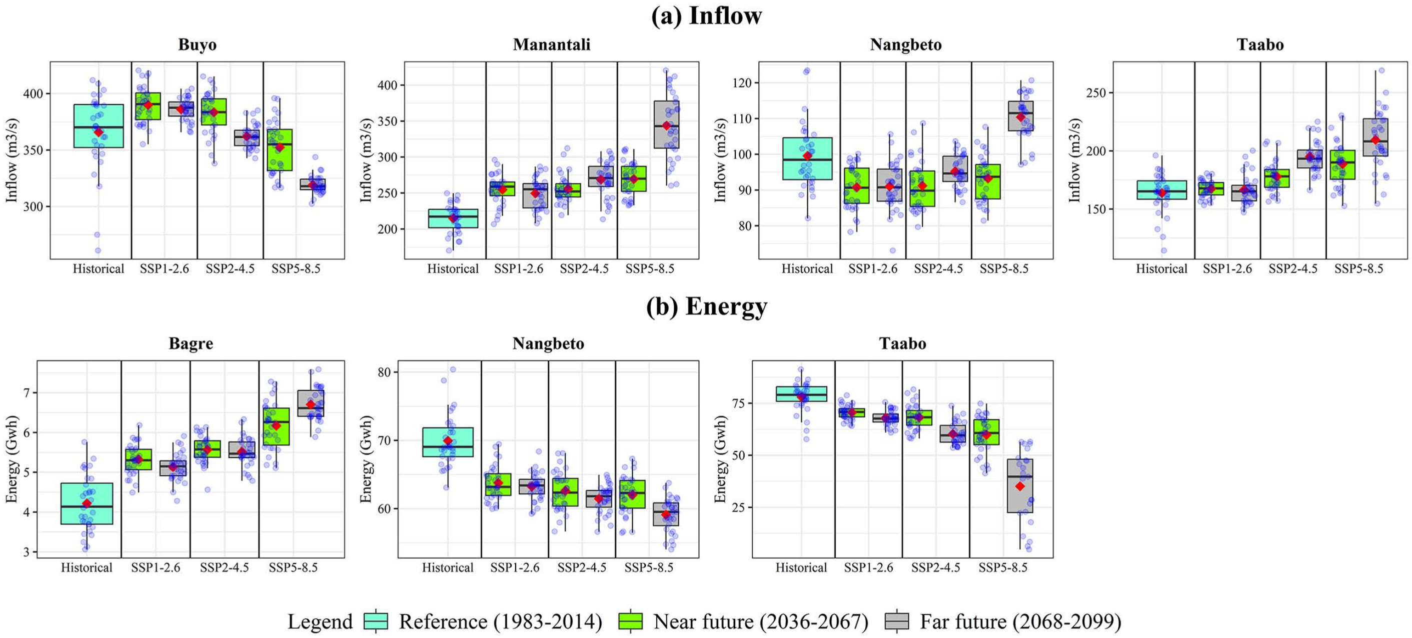

Fig 7. Changes in (a) inflow and (b) energy between the reference and projection periods.

https://doi.org/10.1371/journal.pclm.0000986.g007

comparison of scenarios yielded mixed results. For the Taabo HPP, relative to the reference period, average inflow is projected to increase under SSP5-8.5 scenario for both the near and far futures and under SSP2-4.5 scenario in the far future, with increases not exceeding 19%. Conversely, slight decreases are projected in the near and far futures under SSP1-2.6 scenario and in the near future under SSP2-4.5 scenario, with reductions up to 7%. Relative to the near future, inflow is expected to decrease slightly in the far future under SSP1-2.6 scenario, while increases are projected under the other two scenarios. The comparative analysis of scenarios revealed that SSP5-8.5 consistently projects the highest inflow values, while the results for SSP1-2.6 and SSP2-4.5 are more variable, with one scenario often predicting the lowest values.

For energy projections based on the EnsMean (Fig 7b) relative to the reference period, the Bagre HPP is expected to experience an increase in energy output, while decreases are projected for the Nangbeto and Taabo HPPs. These energy changes are significantly different from the reference period. For the Bagre HPP, all scenarios and projection periods indicate increases, with a maximum rise of 42% under the SSP5-8.5 scenario in the far future. The smallest increase is projected under SSP1-2.6, while SSP5-8.5 consistently predicts the largest increases across both periods. Compared to the near future, a slight decrease is projected in the far future under SSP1-2.6 and SSP2-4.5, while SSP5-8.5 projects a further increase. For the Nangbeto HPP, average energy output is expected to decline compared to the reference period, with reductions of up to 19% in the far future under SSP5-8.5. Similar declines are forecast for both the near and far future under SSP1-2.6 and SSP2-4.5, with a slightly larger reduction in the far future under SSP5-8.5. Scenario comparisons show mixed results, with no single scenario consistently dominating. For the Taabo HPP, significant decreases in average energy output are projected relative to the reference period, reaching up to 58% in the far future under SSP5-8.5. Decreases are consistently projected in the far future compared to the near future across all scenarios. Among the scenarios, SSP1-2.6 predicts the highest average energy values, while SSP5-8.5 forecasts the lowest.

Taken together, the results for both inflow and energy emphasize that climate change impacts on hydropower in West Africa are highly heterogeneous across HPPs, variables, scenarios, and time horizons. No uniform narrative of increasing or decreasing water and energy availability applies across the region. Instead, the findings call for HPP-specific adaptation planning that accounts for the full range of projected changes and their associated uncertainties, including both the risks of inflow and energy declines and the potential opportunities offered by projected increases at specific facilities under certain emission pathways.

4 Discussion

Model performance

Algorithm performance varied depending on the target variables and hydropower plant, except for the Taabo HPP, where svmPoly consistently outperformed others for both inflow and energy predictions. For inflow, the top-performing algorithms were svmRadial for Buyo ($R^2 = 0.9$ and RMSE = 0.007) and Nangbeto ($R^2 = 0.9$ and MAPE = 0.01), and svmPoly for Manantali ($R^2 = 0.95$ and MAPE = 0.054). For energy, the best-performing algorithms were rf for Akosombo ($R^2 = 0.22$ and MAPE = 0.1) and Nangbeto ($R^2 = 0.8$ and MAPE = 0.007), svmPoly for Buyo ($R^2 = 0.51$ and MAPE = 0.01), glmboost for Bagre ($R^2 = 0.63$ and MAPE = 0.043), and ctree for Kpong ($R^2 = 0.2$ and MAPE = 0.2). These variations may stem from differences in the target variables and the ability of certain algorithms to better capture unique patterns. Climatic conditions and geographical factors likely also contributed to the observed performance differences.

Notably, [11] reported different findings in their study on the Nangbeto hydropower dam basin, where ensemble learning with eight algorithms was used to simulate inflow and energy in three steps. In their work, knn was the best-performing algorithm for inflow ($R^2 = 0.82$ and MAPE = 0.093), while gbm performed best for energy ($R^2 = 0.87$ and MAPE = 0.029). For inflow, the five-step ensemble machine learning approach demonstrated superior performance, as indicated by higher R^2 and lower MAPE compared to their study. In contrast, for energy, the five-step approach resulted in a slight reduction in R^2, although predictive accuracy improved, as reflected by a lower MAPE. Although both studies focused on the same area, the discrepancy in results may be due to differences in the number of algorithms used and the chosen value of k ($k = 10$ in this study and $k = 5$ in their study). These results highlight the importance of considering a broader range of algorithms and thoroughly assessing algorithm performance within ensemble learning frameworks before selecting final models. In addition, preliminary tests are necessary to carefully select the value of k.

The five-step ensemble machine learning approach outperformed the physically based hydrological model SWAT in the Manantali hydropower dam basin for inflow simulation. The study by [32] reported Nash-Sutcliffe efficiency (NSE) values below 0.72. This improved performance may reflect the ensemble approach's capacity to capture complex, non-linear hydroclimatic relationships, thereby reducing predictive bias. However, this comparison should be interpreted with caution, as process-based and data-driven models differ fundamentally in their representation of hydrological processes, input requirements, and sensitivity to calibration data. Therefore, the relative benefit of the five-step ensemble machine learning approach is likely contingent on multiple factors: the volume of data used for training, the source and temporal coverage of the input data, and the rigor of parameter calibration within the SWAT framework.

The algorithms demonstrated consistently strong performance for inflow simulation across all layers and hydropower plants, with NSE and R^2 values exceeding 0.6. However, performance for energy simulation varied depending on the layer and hydropower plant. For the final model, NSE and R^2 values greater than 0.6 were achieved for the Bagre, Nangbeto, and Taabo hydropower plants. This variability may be attributed to the complexity of energy simulation compared to inflow. While inflow is heavily influenced by climate variables, making it easier for models to capture these relationships, energy involves additional factors, such as reservoir storage time series, operational rule curves, and demand data, inputs that were unavailable for this study. These results are not indicative of a failure of the ML framework but rather reflect a fundamental identifiability problem: the energy output of these large storage reservoirs is governed by multi-year water balance dynamics, inter-basin transfer operations, and discretionary dispatch decisions.

These findings emphasize that the machine learning models evaluated in this study are highly effective for inflow simulation based on climate variables. However, for energy simulation, careful evaluation of model performance is necessary before application.

Potential sources of limitation

The boxplot range of observations during the reference period was larger than the boxplot range of models and multi-model ensemble mean, regardless of the projection period, target variable, and hydropower plant. Several factors could contribute to this observation. (1) The bias adjustment method: [24] demonstrated that the delta change method aligns the mean with observation, which could reduce the variability and extremes in bias adjusted time series. (2) The scarcity of extreme values in target variables time series: the underrepresentation of extreme values in observation makes them difficult to capture by machine learning models. (3) The high variance of the target variables can complicate the identification of consistent patterns, further challenging the performance of machine learning models. [7] reported similar results when simulating inflow to the Faye hydropower dam using Random Forest, noting model overestimation of minimal inflow and underestimation of maximal inflow. This led to a reduced boxplot range for individual models and the ensemble mean during projections compared to observations from the 1990–2014 reference period.

Like this study, they used a monthly timescale, CHIRPS and CHIRTS data, and the delta change method to bias-adjust thirteen CMIP6 models and multi-model ensemble mean under SSP1-2.6, SSP2-4.5, and SSP5-8.5. With $k=10$ cross-validation and an 80% / 20% train / validation split, their findings, despite differences in approach, location, and models highlight the limited ability of machine learning to capture extremes, likely due to optimization for central conditions and the scarcity of extreme values and high variance.

Climate variability and change impacts on reservoir inflow and energy

The projected hydroclimatic changes across the seven study basins reveal a spatially differentiated vulnerability landscape that does not conform to a simple regional narrative of increasing or decreasing water availability. Projected warming (up to 3.8°C) and slight precipitation increases (< 5%) lead to divergent inflow trends at Nangbeto and Taabo hydropower plants. Nangbeto inflow decreases (up to 13%) except under far-future SSP5-8.5, while Taabo inflow varies, decreasing (max 7%) under SSP1-2.6 but increasing (max 19%) under SSP5-8.5. These contrasting responses are primarily driven by the nonlinear balance between precipitation inputs and temperature-induced evaporative losses. At Nangbeto, increased atmospheric evaporative demand caused by higher temperatures likely exceeds the modest precipitation gains, reducing effective runoff, soil moisture retention, and catchment recharge, which ultimately lowers reservoir inflow. At Taabo, stronger runoff generation under SSP5-8.5 may occur when rainfall intensity compensates for evaporation losses, particularly in wetter years where catchment saturation enhances streamflow transfer to the reservoir. Evaporation effects due to projected warming could explain these trends. Similar findings by [11] over the Nangbeto dam basin reinforce climate-driven hydrological shifts despite methodological differences.

Projected climate changes exhibit distinct patterns across hydropower basins in West Africa. Under SSP1-2.6, Manantali, Nangbeto, and Taabo show consistent warming, slight precipitation declines, and corresponding inflow reductions from the near to far future. In contrast, SSP2-4.5 and SSP5-8.5 scenarios indicate temperature-driven increases in inflow despite slight precipitation declines, with the most pronounced effects under SSP5-8.5. This apparent paradox may reflect the influence of intensified hydrological extremes under warmer climates, where fewer but heavier rainfall events increase direct runoff efficiency even when annual precipitation totals decline slightly. Therefore, inflow sensitivity depends not only on total rainfall amounts but also on rainfall temporal distribution, antecedent soil moisture, and watershed storage dynamics. These findings suggest that inflow sensitivity varies across scenarios, responding more strongly to precipitation under SSP1-2.6 and to temperature under SSP2-4.5 and SSP5-8.5.

At Buyo, projected warming and minimal precipitation changes are expected to reduce inflows, exacerbate drought conditions, increase evaporation, and limit water availability and hydropower generation and heighten the risk of aquatic plant proliferation in the reservoir. The projected inflow declines places Buyo in a high-risk vulnerability category because reduced reservoir levels may lower hydraulic head, directly decreasing turbine efficiency and power generation capacity. The resulting lower water levels may also disrupt downstream hydropower operations at Soubre and Gribo-Popoli. For Buyo, adaptive strategies should include integrated reservoir rule curve optimization, drought contingency storage planning, sediment control, and coordinated cascade dam management to secure downstream flows. Conversely, Manantali is projected to experience inflow increases, benefiting agriculture and hydropower generation but heightening flooding risks and accelerating sedimentation, which could reduce reservoir capacity and alter aquatic ecosystems. For Manantali, adaptation priorities should focus on flood-controlled reservoir releases, sediment flushing operations, and strengthened watershed conservation to reduce erosion from upstream catchments. Given the dual benefit-risk profile, Manantali represents a moderate-risk but high-management-opportunity basin.

Despite projected inflow changes, energy at Nangbeto and Taabo is expected to decline, posing challenges to electricity supply amid rising demand. This indicates that changes in hydropower generation are not solely controlled by inflow volumes but also by reservoir operating levels, timing of inflow relative to electricity demand, and generation efficiency thresholds for turbine functioning. Lower dry-season storage may particularly constrain firm energy production even when annual inflows remain relatively stable. Given that each additional degree of warming can increase electricity consumption by 6–10% in tropical cities [33], projected temperature rises of up to 3.5°C–4°C further complicate energy security. Considering projected energy declines at Nangbeto and Taabo, these systems can be classified as medium-to-high energy security risk zones under future climate stress. Energy planning should therefore prioritize diversification through solar-hydropower hybridization, regional grid interconnection reinforcement, and demand-side efficiency programs to reduce dependence on climate-sensitive hydropower alone. However, Bagre is expected to experience increased energy production, potentially strengthening its role in the regional energy mix and supporting climate change mitigation efforts. Bagre may therefore serve as a strategic balancing asset within regional power pools, compensating for deficits in more vulnerable basins. These findings highlight the urgent need for adaptive water and energy management strategies to balance hydropower sustainability and energy security in a warming climate. From a governance perspective, stronger transboundary water coordination, climate-informed dam operation policies, and flexible allocation frameworks will be essential to manage competing demands among hydropower, irrigation, flood control, and ecosystem services across West African river basins.

5 Conclusion

This study developed a novel five-step ensemble machine learning approach to improve the assessment of climate change impacts on inflow and hydropower generation across seven West African dam basins (Akosombo, Bagre, Buyo, Kpong, Manantali, Nangbeto, and Taabo). By using five successive layers and gradually refining the model structure, the proposed approach enhances predictive robustness compared to conventional modeling frameworks. The best model was used for projecting inflow and energy using delta bias-adjusted CMIP6 models under SSP1-2.6, SSP2-4.5 and SSP5-8.5. Model performance at each step was evaluated using R^2, NSE, MAPE and nRMSE.

The ensemble framework delivered reliable inflow simulation performance across all layers and HPPs, with R^2 and NSE consistently exceeding 0.6. Energy modeling revealed greater site-dependency, with satisfactory performance (R^2 and NSE > 0.6) achieved at Bagre, Nangbeto, and Taabo.

Projections indicate a consistent rise in temperature (up to 4.5°C), combined with heterogeneous precipitation changes. These climatic shifts are projected to lead to significant inflow reductions at Buyo (by up to 24%), Nangbeto (by up to 13%), and Taabo (by up to 7%). However, Manantali is projected to experience potential increases. Energy production is projected to decline at Nangbeto and Taabo (by up to 19% and 58%, respectively), whereas Bagre may experience gains of up to 42%. For Nangbeto, precipitation increases (≤ 5%) and temperature rises (≤ 3.5°C) are expected to reduce inflows by up to 10% and energy output by 42%. Similarly, at Taabo, projected precipitation increases (≤ 5%) and temperature rises (≤ 3.8°C) may decrease inflows by up to 7% under SSP1-2.6 and SSP2-4.5 in the near term, while potential inflow increases (≤ 19%) are projected under SSP2-4.5 (long-term) and SSP5-8.5. However, Taabo's hydropower is expected to decline by up to 58%, highlighting a substantial risk to regional electricity supply. Overall, the findings reveal strong spatial variability in climate change impacts on hydropower across West Africa, emphasizing that future energy production will not respond uniformly to climate forcing. This highlights the vulnerability of certain hydropower systems and the need for differentiated adaptation strategies.

From a practical perspective, projected reductions in hydropower generation could increase pressure on existing infrastructure and potentially lead to greater reliance on thermal energy sources, thereby undermining climate mitigation efforts. These results underline the importance of integrating climate risks into energy planning, strengthening reservoir management, and diversifying renewable energy portfolios.

These findings provide a robust and scalable methodological framework, along with new regional insights into hydropower vulnerability under climate change. It offers valuable guidance for policymakers and stakeholders aiming to enhance energy security and climate resilience in West Africa.

Future research should address several limitations of the present framework. The integration of reservoir storage time series, operational rule curves, and electricity demand data as additional predictors could substantially improve energy simulation performance, particularly for large storage facilities such as Akosombo and Kpong. Combining the present data-driven framework with process-based hydrological models in a hybrid modeling structure could leverage the complementary strengths of both approaches. The physical interpretability of process-based models and the pattern-recognition efficiency of ML, to produce more reliable and actionable hydropower vulnerability assessments for West Africa.

Supporting information

S1 Fig. Precipitation and temperature projection for the Akosombo basin.
(TIF)

S2 Fig. Precipitation and temperature projection for the Bagre basin.
(TIF)

S3 Fig. Precipitation and temperature projection for the Buyo basin.
(TIF)

S4 Fig. Precipitation and temperature projection for the Kpong basin.
(TIF)

S5 Fig. Precipitation and temperature projection for the Manantali basin.
(TIF)

S6 Fig. Precipitation and temperature projection for the Nangbeto basin.
(TIF)

S7 Fig. Precipitation and temperature projection for the Taabo basin.
(TIF)

S8 Fig. Changes in inflow to the Buyo HP dam.
(TIF)

S9 Fig. Changes in inflow to the Manantali HP dam.
(TIF)

S10 Fig. Changes in inflow to the Nangbeto HP dam.
(TIF)

S11 Fig. Changes in inflow to the Taabo HP dam.
(TIF)

S12 Fig. Changes in energy produced by the Bagre HPP.
(TIF)

S13 Fig. Changes in energy produced by the Nangbeto HPP.
(TIF)

S14 Fig. Changes in inflow to the Taabo HP dam.
(TIF)

S1 Data. S1 Data includes two folders. The first, HINDCAST, contains CHIRPS and CHIRTS data covering the study period, together with raw CMIP6 model outputs. The second, BIAS-ADJUSTED_CLIM_MODEL, provides Delta bias-adjusted climate model simulations prepared for comparative analysis.
(RAR)

S1 Code. S1 Code provides the R scripts used to conduct the analyses and generate the figures presented in the paper.
(RAR)

Acknowledgments

The authors thank the Institute of Research for Development (IRD, France), the Compagnie Ivoirienne d'Electricité (CIE), the Joint International Laboratory (LMI-NEXUS) and the Laboratory of Matter, Environment and Solar Energy Sciences (LASMES) of Felix Houphouët Boigny University (UFHB, Côte d'Ivoire), the African Centre of Excellence on Climate Change, Biodiversity and Sustainable Agriculture (CEA-CCBAD/WASCAL, Côte d'Ivoire) for providing the facility, technical and scientific assistance to perform this study. The authors thank also the National Computing Center of Côte d'Ivoire (CNCCI) for supporting and providing the facility (the Climate Modelling Platform).

Author contributions

Conceptualization: Salomon Obahoundje.

Data curation: Salomon Obahoundje, Dior Diallo, Ernest Amoussou, Daniel Yamegueu, Eric Antwi Ofosu.

Formal analysis: Franck Hervé Akaffou.

Funding acquisition: Salomon Obahoundje, Arona Diedhiou.

Investigation: Franck Hervé Akaffou.

Methodology: Franck Hervé Akaffou, Salomon Obahoundje.

Project administration: Salomon Obahoundje.

Supervision: Arona Diedhiou, Kouakou Lazare Kouassi, Ernest Amoussou.

Validation: Salomon Obahoundje.

Visualization: Franck Hervé Akaffou.

Writing – original draft: Franck Hervé Akaffou.

Writing – review & editing: Franck Hervé Akaffou, Salomon Obahoundje, Dior Diallo, Ernest Amoussou, Daniel Yamegueu, Eric Antwi Ofosu.

References

1. IHA. 2024 World hydropower outlook: opportunities to advance net zero [Internet]. Canada: International Hydropower Association; 2024. 96 p. Available via: https://www.hydropower.org/publications/2024-world-hydropower-outlook
2. IHA. Hydropower statut report [Internet]. 2020. 54 p. Available via: https://www.hydropower.org/publications/2020-hydropower-status-report
3. Obahoundje S, Diedhiou A, Akpoti K, Kouassi KL, Ofosu EA, Marcel Kouame DG. Predicting climate-driven changes in reservoir inflows and hydropower in Côte d'Ivoire using machine learning modeling. Energy. 2024;302(131849):1–14. https://doi.org/10.1016/j.energy.2024.131849
4. Obahoundje S, Diedhiou A. Potential impacts of climate, land use and land cover changes on hydropower generation in West Africa: a review. Environ Res Lett. 2022;17:1–20. https://doi.org/10.1088/1748-9326/ac5b3b
5. Almazroui M, Saeed F, Saeed S, Nazrul Islam M, Ismail M, Klutse NAB, et al. Projected Change in Temperature and Precipitation Over Africa from CMIP6. Earth Syst Environ. 2020;4(3):455–75. https://doi.org/10.1007/s41748-020-00161-x
6. Quenum GMLD, Nkrumah F, Klutse NAB, Sylla MB. Spatiotemporal Changes in Temperature and Precipitation in West Africa. Part I: Analysis with the CMIP6 Historical Dataset. Water. 2021;13(24):3506. https://doi.org/10.3390/w13243506
7. Akaffou FH, Obahoundje S, Didi SRM, Koffi B, Coulibaly WB, Habel M, et al. Analyzing inflow to Faye reservoir sensitivity to climate change using CMIP6 and random forest algorithm. Int J River Basin Manag. 2025;23(4):589–608. https://doi.org/10.1080/15715124.2024.2354707
8. Zhou T, Kao SC, Xu W, Gangrade S, Voisin N. Impacts of climate change on subannual hydropower generation: a multi-model assessment of the United States federal hydropower plant. Environ Res Lett. 2023;18(3):1–14. https://doi.org/10.1088/1748-9326/acb58d
9. Jung J, Han H, Kim K, Kim HS. Machine learning-based small hydropower potential prediction under climate change. Energies. 2021;14(12):1–10. https://doi.org/10.3390/en14123643
10. Kartal V. Machine learning-based streamflow forecasting using CMIP6 scenarios: assessing performance and improving hydrological projections and climate change. Hydrol Process. 2024;38(6):1–24. https://doi.org/10.1002/hyp.15204
11. Obahoundje S, Diedhiou A, Dubus L, Adéchina Alamou E, Amoussou E, Akpoti K, et al. Modeling climate change impact on inflow and hydropower generation of Nangbeto dam in West Africa using multi-model CORDEX ensemble and ensemble machine learning. Appl Energy. 2022;325:119795. https://doi.org/10.1016/j.apenergy.2022.119795
12. Mul M, Obuobie E, Appoh R, Kankam-Yeboah K, Bekoe-Obeng E, Amisigo B, et al. Water resources assessment of the Volta River Basin [Working paper] [Internet]. Working paper no.: 166. Accra, Ghana: International Water Management Institute (IWMI); 2015 [cité 13 nov 2024]. 82 p. Available via:https://hdl.handle.net/10568/75719
13. Koua BK, Koffi PME, Gbaha P, Touré S. Present status and overview of potential of renewable energy in Cote d'Ivoire. Renew Sustain Energy Rev. 2015;41:907–14. http://dx.doi.org/10.1016/j.rser.2014.09.010
14. Ouedraogo Y, Yamegueu D, Fowe Tazen L, Leye B, Bologo Traore M, Konda M. Addressing the Water-Energy-Food Nexus in the Context of Climate Change: The Case of Bagré Dam in Burkina Faso. Sci Afr. 2024;24:1–12. https://doi.org/10.1016/j.sciaf.2024.e02251
15. Obahoundje S, Assoumou E, Youan Ta M, Kouassi KL, Diedhiou A. Multiyear rainfall variability in the Mono river basin and its impacts on Nangbeto hydropower scheme. In: Proceedings IAHS. 2021. p. 343–7.
16. Faye JM, Ndao S, Sambou LEV. Management of significant environmental aspects and impacts in accordance with the ISO 14001:2015 standard during the operation and maintenance phase of Senegal River Basin Development Authority hydroelectric works and facilities: The case of Manantali Dam. GEP. 2024;12(10):89–110. https://doi.org/10.4236/gep.2024.1210006
17. Sacré Regis M. D, Mouhamed L, Kouakou K, Adeline B, Arona D, Houebagnon Saint. J. C, et al. Using the CHIRPS Dataset to Investigate Historical Changes in Precipitation Extremes in West Africa. Climate. 2020;8(84):84. https://doi.org/10.3390/cli8070084
18. Koffi B, Brou AL, Kouadio KJO, Ebodé VB, N'guessan KJY, Yangouliba GI, et al. Impact of climate and land use/land cover change on Lobo reservoir inflow, West-Central of Côte d'Ivoire. J Hydrol Reg Stud. 2023;47(101417):101417. https://doi.org/10.1016/j.ejrh.2023.101417
19. Verdin A, Funk C, Peterson P, Landsfeld M, Tuholske C, Grace K. Development and validation of the CHIRTS-daily quasi-global high-resolution daily temperature data set. Sci Data. 2020;7(1):303. https://doi.org/10.1038/s41597-020-00643-7 PMID: 32929097
20. Bigot S, Dumas D, Brou TY, Noufe DD, Dibi P, N'Da KC, et al. Climate projections CMIP6 at the scale of southeast Côte d'Ivoire: Evolution of thermo-pluviometric constraints for the main agrosystems involving cocoa, rubber, oil palm, and cassava. In: 35ème colloque annuel de l'Association Internationale de Climatologie. Toulouse, France; 2022. p. 60–6.
21. Dong Z, Liu H, Baiyinbaoligao, Hu H, Khan MYA, Wen J, et al. Future projection of seasonal drought characteristics using CMIP6 in the Lancang-Mekong River Basin. J Hydrol. 2022;610(127815):127815. https://doi.org/10.1016/j.jhydrol.2022.127815

22. Hua L, Zhao T, Zhong L. Future changes in drought over Central Asia under CMIP6 forcing scenarios. J Hydrol. 2022;43(101191):101191. https://doi.org/10.1016/j.ejrh.2022.101191

23. Saha U, Sateesh M. Rainfall extremes on the rise: observations during 1951–2020 and bias-corrected CMIP6 projections for near- and late 21st century over Indian landmass. J Hydrol. 2022;608(127682):127682. https://doi.org/10.1016/j.jhy

24. Navarro-Racines C, Tarapues J, Thornton P, Jarvis A, Ramirez-Villegas J. High-resolution and bias-corrected CMIP5 projections for climate change impact assessments. Sci Data. 2020;7(1):7. https://doi.org/10.1038/s41597-019-0343-8 PMID: 31959765

25. Zhang Y, Liu J, Shen W. A review of ensemble learning algorithms used in remote sensing applications. Appl Sci. 2022;12(17):1–20. https://doi.org/10.3390/app12178654

26. Nti IK, Adekoya AF, Weyori BA. A comprehensive evaluation of ensemble learning for stock-market prediction. J Big Data. 2020;7(1). https://doi.org/10.1186/s40537-020-00299-5

27. Ho LTT, Dubus L, De Felice M, Troccoli A. Reconstruction of Multidecadal Country-Aggregated Hydro Power Generation in Europe Based on a Random Forest Model. Energies. 2020;13(7):1786. https://doi.org/10.3390/en13071786

28. Kraisangka J, Rittima A, Sawangphol W, Phankamolsil Y, Tabucanon AS, Talaluxmana Y, et al. Application of Machine Learning in Daily Reservoir Inflow Prediction of the Bhumibol Dam, Thailand. In: 2022 19th International Conference on Electrical Engineering/Electronics, Computer, Telecommunications and Information Technology (ECTI-CON). 2022. p. 1–4.

29. Kordi-Karimabadi F, Fadaei-Kermani E, Ghaeini-Hessaroeyeh M, Farhadi H. Integrating numerical models with deep learning techniques for flood risk assessment. Sci Rep. 2025;15(1):8913. https://doi.org/10.1038/s41598-025-93465-9 PMID: 40087490

30. Yue Z, Wang L, Zhu J, Zhou H. Comparative Study of Shallow and Deep Learning-Based Data-Driven Models for Monthly Runoff Simulation in the Yalong River Basin. Water. 2025;17(18):2735. https://doi.org/10.3390/w17182735

31. Chen W, Nguyen KA, Lin BS. Rethinking evaluation metrics in hydrological deep learning: insights from torrent flow velocity prediction. Sustain. 2025;17(19):8658. https://doi.org/10.3390/su17198658

32. Sambou S, Sane ML, Leye I, Ndione DM, Kane S, Badji ML. Calage et validation de SWAT sur le bassin versant du Bafing (Fleuve Sénégal) en amont de BAFING MAKANA: vers une application à la gestion du barrage de Manantali. Proc IAHS. 2021;384:363–6. https://doi.org/10.5194/piahs-384-363-2021

33. Kondi-Akara G, Hingray B, Francois B, Diedhiou A. Recent trends in urban electricity consumption for cooling in West and Central African countries. Energy. 2023;276:127597. https://doi.org/10.1016/j.energy.2023.127597